

# A flame-retardant-free and thermo-cross-linkable copolyester: Flame-retardant and anti-dripping mode of action



Hai-Bo Zhao, Bo-Wen Liu, Xiao-Lin Wang, Li Chen\*, Xiu-Li Wang, Yu-Zhong Wang\*

Center for Degradation and Flame-Retardant Polymeric Materials, College of Chemistry, State Key Laboratory of Polymer Materials Engineering, National Engineering Laboratory of Eco-Friendly Polymeric Materials (Sichuan), Sichuan University, Chengdu 610064, PR China

## ARTICLE INFO

### Article history:

Received 24 January 2014

Received in revised form

20 March 2014

Accepted 22 March 2014

Available online 31 March 2014

### Keywords:

Cross-linking

Flame retardance

Anti-dripping

## ABSTRACT

Flame-retardant-free and thermo-cross-linkable copolyesters have been synthesized, and their flame retardation and anti-dripping behavior as a consequence of cross-linking during combustion were investigated in detail. TG-DSC simultaneous thermal analysis, rheological analysis, and TGA established the extent and rate of the cross-linking reaction. The extent of cross-linking depends on the content of cross-linkable monomer, PEPE, and the higher the extent of the cross-linking, the better the flame retardance and anti-dripping performance of copolyesters. The large melt viscosity caused by cross-linked networks at high temperature played the most important role in anti-dripping of copolyesters. TG-FTIR results confirmed that the flame-retardant activity of copolyesters mainly took effect in the condensed phase, and XPS results indicated that the carbonization process was aromatization-dominant. SEM and Raman analysis suggested that the char layers were constituted mainly of polyaromatic species with small and uniform microstructures at the surface. Consequently, both the large melt viscosity and the formation of an especially compact char with fine microstructure resulting from cross-linking were considered as the key to the flame retardance and anti-dripping performance of the polymer when subjected to the flame.

© 2014 Elsevier Ltd. All rights reserved.

## 1. Introduction

In the modern polymer industry, a variety of polymerization methods are used to fabricate sundry and specialty plastics, foams, fibers and rubbery materials. These polymers change society and bring great convenience to human life. Despite many benefits from these polymers, many imperfections remain problematic, and the fire risk from use of polymers may seriously threaten lives and property of humans. Due to the widespread use of polymer materials, it is necessary and important to make most polymers non-flammable. Fire-related issues continue to drive the development of polymers that reduce fire risk to save lives and protect property [1]. To flame-retard those polymeric materials, conventional methods are to incorporate some flame-retardant elements into their main chains or side chains, or to add some flame retardants to their matrices [2]. However, any flame retardants used to reduce fire risk must conform to various safety standards to prevent harm to the ecological environment and human health. Based on this

concept, some traditional halogenated flame retardants are banned in many countries [3]. World-wide interest in halogen-free flame retardants has been increasing, and many other flame retardant materials containing elements such as P, N, S and Si are being used to flame-retard polymer materials [4–9]. These flame retardants are considered to be of relatively low toxicity. Whether or not they can meet future environmental and health standards is uncertain. If a polymer could display flame resistance despite the absence of any flame retardant element (say, bromine, chlorine, phosphorus, or nitrogen, etc.), it may be truly green and environment-friendly. However, there have been few reports of flame-retarded polymers containing no flame-retardant elements [10,11].

Recently, a smart cross-linkable PET-based copolyester P(ET-co-P) formed with only carbon, hydrogen, and oxygen had been synthesized [12]. This copolyester exhibited no reactivity at the temperature of synthesis and processing but could cross-link rapidly at higher temperature before burning. The self-extinguishment and anti-dripping behavior of the polyester could be achieved through cross-linking during burning. Despite the absence of any traditional flame-retarding element, this high-temperature cross-linking may provide a new strategy for the formation of a flame-retardant system without the need for the presence of any flame-retardant element. Thus, it is important to understand the specific

\* Corresponding authors. Tel./fax: +86 28 85410755.

E-mail addresses: [l.chen.scu@gmail.com](mailto:l.chen.scu@gmail.com) (L. Chen), [yzwang@scu.edu.cn](mailto:yzwang@scu.edu.cn), [polymers@126.com](mailto:polymers@126.com) (Y.-Z. Wang).

relationship between cross-linking and flame retardation as well as anti-dripping. The flame retardance affected by cross-linking has been investigated in detail. Simultaneously, to highlight the flame-retardant effect of cross-linking, more functional cross-linkable monomers (PEPE) were incorporated into the copolyesters via melt polycondensation, and the flame-retardant properties of those more highly cross-linkable polymers were investigated [13].

## 2. Experimental

### 2.1. Chemicals and substrates

4-Phenylethynylphthalic anhydride (PEPA) was purchased from Changzhou Sunlight Pharmaceutical Co., Ltd. (Changzhou, China). Antimony trioxide ( $\text{Sb}_2\text{O}_3$ , AR), ethylene glycol (EG), dimethyl terephthalate (DMT), methanol, phenol, tetrachloroethane, hexafluoro isopropanol, zinc acetate (CP) were all manufactured by Chengdu Chemical Industries Co. (Chengdu, China) and used as received.

### 2.2. Sample preparation

Poly(ethylene terephthalate-co-4-phenylethynylphthalate) abbreviated as P(ET-co-P)s were synthesized using established procedures [12]. The preparation of P(ET-co-P)<sub>40</sub> is presented here as a representative example, where the number 40 denotes the molar parts of PEPE per hundred of DMT (say, PEPE: DMT = 40: 100 in mol). 44.4 g (0.229 mol) DMT, 35.5 g (0.573 mol) EG and 0.0799 g ( $4.35 \times 10^{-4}$  mol) zinc acetate were added to a 250-mL bottle equipped with a Dean–Stark trap with a condense. The reaction system was firstly heated to 180 °C for 3 h. As the reaction proceeded, methanol was released. After a stoichiometric amount of methanol was removed, the mixture was poured into an excess of warm water, and the precipitate bis(2-hydroxyethyl) terephthalate (BHET) was obtained. The precipitate was filtrated, washed by water, and dried overnight. Then, stoichiometric BHET (0.229 mol) was added to a 250 mL polymerization bottle. And ethylene glycol solution of PEPE/PEPA (0.0916 mol) and antimony trioxide ( $3.43 \times 10^{-4}$  mol, 0.100 g) was also added. The mixture was heated to 240 °C for 2 h under a steady stream of nitrogen. Finally, the pressure in the vessel was reduced to lower than 60 Pa and the temperature was raised to 270 °C over 0.5 h and maintained for 2–4 h. Other examples were obtained in a similar way. IR (KBr): 2882–2997 (w), 1722 (s), 2210 (m). <sup>1</sup>H NMR ( $\text{CF}_3\text{COOD}$ ,  $\delta$ ): 7.7 (Ar–H in terephthalic and isophthalic structural units), 6.7–7.4 (Ar–H in the 4-phenylethynyl structural unit) and 4.1–4.4 (–CH<sub>2</sub>O). Basic characteristics of the copolyesters are listed in Table 1.

Cross-linked specimens for testing were obtained from the copolyester heated in a muffle furnace at 320 °C ( $\pm 3$  °C) for 60 min in air.

Samples were prepared at different temperatures for XPS tests in a tube furnace in nitrogen. The samples were heated to each specific temperature at a heating rate of 10 °C min<sup>-1</sup>, and the sample was held isothermal for 10 min at each temperature: 330 °C, 380 °C, 430 °C and 550 °C ( $\pm 3$  °C), respectively.

**Table 1**  
Basic characteristics, LOI and UL-94 for neat PET and P(ET-co-P) copolyesters.

Samples	PEPE content (mol%)		$[\eta]$ (dL g <sup>-1</sup> )	LOI	UL-94
	Calculated	Test <sup>a</sup>			
PET	–	–	0.68	22.0	NR
P(ET-co-P) <sub>20</sub>	16.7	16.3	1.17	24.5	V-2
P(ET-co-P) <sub>40</sub>	28.6	28.0	1.24	28.0	V-2
P(ET-co-P) <sub>60</sub>	37.5	36.7	1.49	29.0	NR
P(ET-co-P) <sub>80</sub>	44.4	44.7	1.87	30.0	V-0

<sup>a</sup> Testing results were calculated from NMR.

### 2.3. Characterization

NMR spectra (1H, 400 MHz) were obtained at room temperature using a Bruker AVANCE AVII 400 NMR instrument, with  $\text{CF}_3\text{COOD}$  as the solvent, and tetramethylsilane as the internal reference. Fourier transform infrared spectroscopy (FTIR) was performed using a Nicolet 6700 spectrometer. The intrinsic viscosities of copolyesters were determined with an Ubbelodhe viscometer with a concentration of 0.5 g/dL at 25 °C in 1:1 (v/v) phenol-1, 1, 2, 2-tetrachloroethane solution.

Cross-linking behavior was examined using a NETZSCH simultaneous TGA-DSC (449C) with  $\pm 0.1$  °C temperature error at a heating rate of 10 °C min<sup>-1</sup> in N<sub>2</sub>.

Dynamic oscillatory rheological measurements for neat PET and copolyesters were performed with a parallel-plate fixture (25 mm diameter and 1 mm thickness) using an Advanced Dynamic Rheometric Expansion System (ARES, Bohlin Gemini 200) in an oscillatory shear mode. Temperature scanning tests at a fixed frequency of 0.1 Hz were in the range from 230 °C, 170 °C, 170 °C, and 260 °C to 330 °C for P(ET-co-P)<sub>20</sub>, P(ET-co-P)<sub>40</sub>, P(ET-co-P)<sub>80</sub>, and neat PET, respectively. The temperature error is about  $\pm 1$  °C. Time scanning tests at a fixed frequency of 0.1 Hz were performed at a fixed 300 °C for 550 s.

Thermal decomposition behavior of the copolyesters was conducted using a NETZSCH TGA (209 F1) with  $\pm 0.1$  °C temperature error at a heating rate of 10 °C min<sup>-1</sup>.

Thermogravimetric analysis-infrared spectrometry (TG-IR) was performed using the NETZSCH TGA (209 F1) thermogravimetric analyzer that was linked to the Nicolet 6700 FTIR spectrophotometer. The heating rate was 10 °C min<sup>-1</sup> from 40 °C to 700 °C (nitrogen atmosphere, flow rate of 50 ml/min).

Heat release rate (HRR), total heat release (THR), and the burning residues were measured using an FTT cone calorimeter according to ISO 5660-1 at a heat flux 50 kW/m<sup>2</sup>. The samples were molded to size of 100 × 100 × 3 mm<sup>3</sup>. The molding temperature was 260 °C, 210 °C, 200 °C, 200 °C, 200 °C for PET, P(ET-co-P)<sub>20</sub>, P(ET-co-P)<sub>40</sub>, P(ET-co-P)<sub>60</sub>, P(ET-co-P)<sub>80</sub> respectively. The experiment error of cone is about  $\pm 10\%$ .

The limiting oxygen index (LOI) values ( $\pm 0.5$ ) were performed using an HC-2C oxygen index measurement (Jiangning, China) with sheet dimensions of 130 × 6.5 × 3.2 mm<sup>3</sup> according to ASTM D 2863-97. The samples were compression molded at 10 MPa and then cut to a size of 130 × 6.5 × 3.2 mm<sup>3</sup>.

The UL-94 vertical test was performed using a vertical burning test instrument (CZF-2) according to ASTM D 3801. The samples were compression molded at 10 MPa and then cut to a size of 125 × 12.7 × 3.2 mm<sup>3</sup>.

X-ray photoelectron spectroscopy (XPS) was carried out with XSAM 800 spectrometer (Kratos Co., UK), using Al K $\alpha$  excitation radiation (1486.6 eV), operated at 12 kV and 15 mA. Binding energies were referenced to the carbonaceous carbon at 285.0 eV.

The microstructures of the residual char collected after the cone calorimeter tests were observed using scanning electron microscopy (JEOL JSM 5900LV) with an acceleration voltage of 10 kV. A thin layer of gold was sprayed at the surface prior to SEM observation.

Raman spectroscopy measurement was carried out at room temperature with LabRAM HR800 laser Raman spectrometer (SPEX Co., USA) using a 532 nm helium-neon laser line.

## 3. Results and discussion

### 3.1. Flammability and anti-dripping behaviors

The flammability of copolyesters has been widely evaluated by cone calorimeter testing [14,15]. Fig. 1 contains cone calorimetric

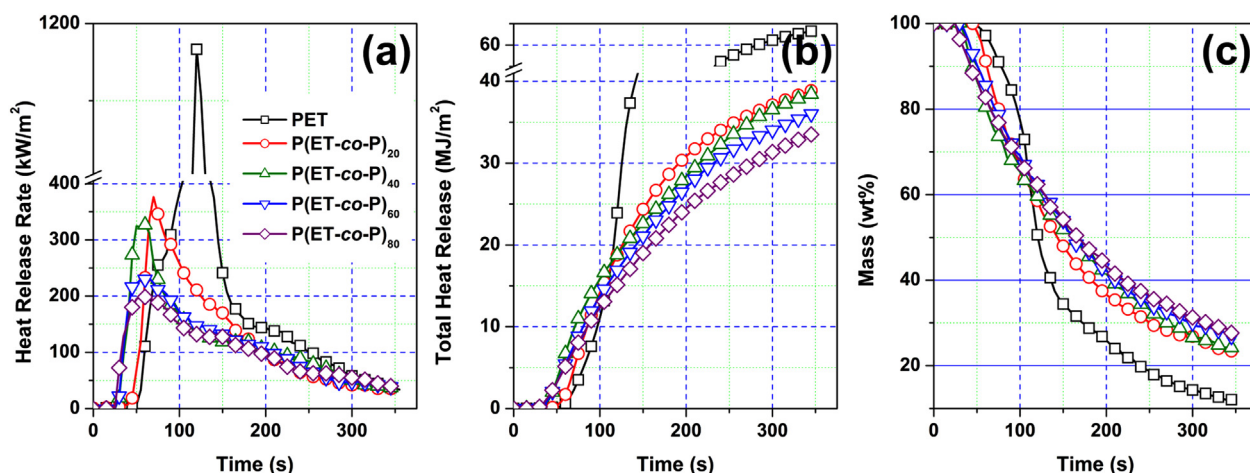


Fig. 1. Cone calorimetric results for PET and P(ET-co-P) copolyesters at an external heat flux of 50 kW m<sup>-2</sup> as function of burning duration: (a) heat release rate, (b) total heat release and (c) residue mass.

results for PET and P(ET-co-P) copolyesters, and the detailed data were summarized in Table 2. The evolution of heat release rate (HRR), especially its maximum value (PHRR) is a very important parameter, indicating the rate of fuel feeding during the combustion and the rate of further flame spread [16,17]. Lower PHRR denotes a slower flame spread and minor fire hazard. From Fig. 1, the introduction of PEPE significantly reduced both the peak and average values of HRR of the copolyesters: PHRR of P(ET-co-P)<sub>20</sub> was about 376 kW m<sup>-2</sup>, decreased to 32% of that of PET; while for P(ET-co-P)<sub>80</sub>, PHRR was only 198 kW m<sup>-2</sup>. Thus, it was clear that PEPE could effectively reduce the HRR of copolyesters and slow the flame propagation. Also, with the incorporation of the functional monomer, the total heat release (THR) of the copolyesters decreased with the increase of PEPE content: the value for neat PET was 63.5 MJ m<sup>-2</sup>; while the values for P(ET-co-P)<sub>20</sub>, P(ET-co-P)<sub>40</sub>, P(ET-co-P)<sub>60</sub> and P(ET-co-P)<sub>80</sub> were 39.0, 38.6, 36.7 and 35.5 MJ m<sup>-2</sup>, respectively. Slow burning of copolyesters could also be observed from the mass loss rate curves (Fig. 1(c)), which were similar to the THR ones. It was noteworthy that with an increase in PEPE content, further suppression of the heat release was not as great as the copolyester with low content of the functional monomer did. We can imagine that the relatively high combustion intensity during cone calorimetry, which resulted in variables such as heat, onsite temperature, volatile free radicals, etc., could accelerate the cross-linking reaction between the phenylethynyl moieties; PEPE was very reactive after ignition, and an expected flame-retardant effect could be achieved at a comparatively low content of PEPE.

Table 2  
Detailed combustion results for neat PET and P(ET-co-P) copolyesters obtained from cone calorimetry.

Samples	PET	P(ET-co-P) <sub>20</sub>	P(ET-co-P) <sub>40</sub>	P(ET-co-P) <sub>60</sub>	P(ET-co-P) <sub>80</sub>
TTI (s) <sup>a</sup>	48	38	23	24	28
PHRR (kW m <sup>-2</sup> )	1167	376	329	232	198
Time to PHRR (s)	120	70	60	65	65
FIGRA (kW m <sup>-2</sup> s <sup>-1</sup> ) <sup>b</sup>	9.7	5.4	5.5	3.6	3.0
Averaged HRR (kW m <sup>-2</sup> )	205	126	119	108	94
THR (MJ m <sup>-2</sup> )	63.5	39.0	38.6	36.7	35.5
Residue (wt%)	11	23	24	26	28

<sup>a</sup> TTI stands for the time to ignition.

<sup>b</sup> FIGRA is calculated by dividing the value of PHRR by the time to PHRR.

Limiting oxygen index (LOI) and vertical burning rate (UL-94), as classical flame-retardant tests, are simple and important methods to evaluate the flammability of polymeric materials, and also provide information about melt dripping of the testing materials [18]. Generally speaking, materials exhibiting LOI values above 26 would show self-extinguishing behavior in air and be considered to possess high flame retardance [19,20]. From LOI data shown in Table 1, it could be easily concluded that the incorporation of PEPE considerably increased the LOI values of copolyesters: the value for neat PET was only 22.0; while the values for P(ET-co-P)<sub>20</sub>, P(ET-co-P)<sub>40</sub>, P(ET-co-P)<sub>60</sub> and P(ET-co-P)<sub>80</sub> were 24.5, 28.0, 29.0 and 30.0, respectively. After combustion, the residue of pure PET was almost all the melting matrix rather than char at the surface; while P(ET-co-P)s showed no melts but compact char, which played a positive role on anti-dripping.

The UL-94 vertical burning test is another important measurement to investigate flammability and melt-dripping behaviors of materials. Different from the behavior in cone and LOI tests, the copolyesters showed great flame retardance only at high content of PEPE in the UL-94 test. As shown in Table 1, P(ET-co-P)s with relatively low content of PEPE failed to pass UL-94 tests, although the tendency of melt dripping during combustion was much depressed with the incorporation of PEPE. However, when more PEPE was copolymerized, an exciting results were found: P(ET-co-P)<sub>80</sub> could reach V-0, and no droplet was found throughout the testing process. The combustion processes for PET and P(ET-co-P)<sub>80</sub> during the UL-94 vertical burning testing are recorded in Fig. 2. For neat PET, the cotton was ignited by melt dripping after the first ignition, and the sample continued to burn with serious dripping and no extinguishing after the second ignition. By contrast, P(ET-co-P)<sub>80</sub> was seen to extinguish quickly following the removal of the igniter (extinguished within 5s for twice ignition), and no dripping was found during the course of the test. After testing, P(ET-co-P)<sub>80</sub> left compact and intumescent char on the bottom of the sample, which prevented dripping and maintained its shape effectively.

It is noteworthy that there are different performances in cone calorimetric, LOI and UL-94 tests for copolymers with various PEPE content. This could be caused by the different combustion intensity and test methods used. In cone calorimetric analysis, the testing samples are supported by a platform, and the effect of gravity on the combustion is weak. Also, the samples are ignited by the persistent external heat irradiation and are under irradiation for a long time, which would keep samples for a long-term cross-linking.

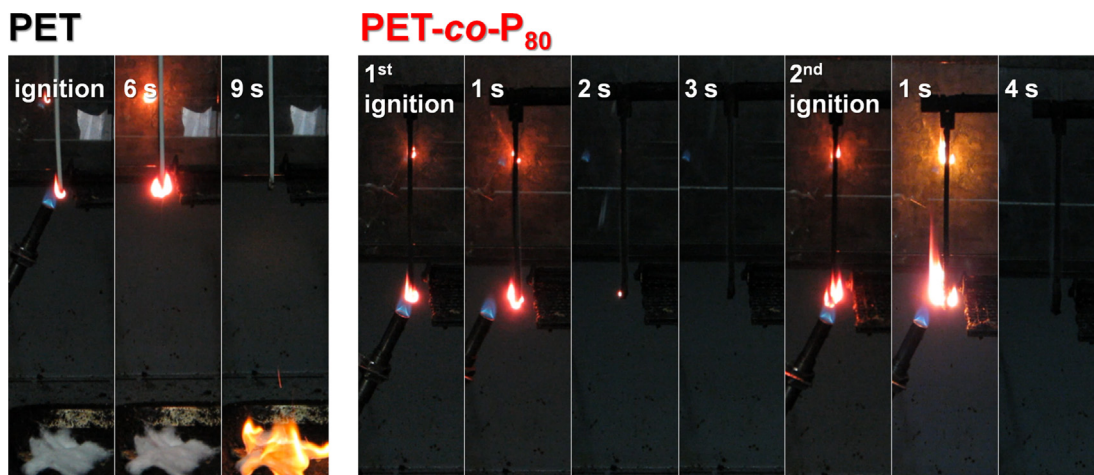


Fig. 2. Combustion processes of PET and P(ET-co-P)<sub>80</sub> during the UL-94 testing at different time.

Thus, 16.3 mol% of PEPE (P(ET-co-P)<sub>20</sub>) can lead to a considerable improvement by decreasing the PHRR from over 1000 to 376 kW m<sup>-2</sup>. In the LOI test, the testing samples are placed vertically by a fixture and ignited at the top. It would be ignited in a very short firing time, while the weight of sample is supported by itself during combustion. For the short cross-linking time, 28.0 mol% of PEPE (P(ET-co-P)<sub>40</sub>) is needed to improve the LOI value of the copolyester. However, in the UL-94 test, the testing samples are ignited at the bottom for 10 s, very close to the firing time of LOI test but much shorter than that of cone calorimetry. Furthermore, the gravity of the sample would trigger the occurrence of melt dripping and promote the spread of fire. As a result, in a short cross-linking time, 44.7 mol% of PETE (P(ET-co-P)<sub>80</sub>) is needed to prevent melt dripping and extinguish fire within an expected time.

### 3.2. Cross-linking behaviors

To elucidate clearly the course of cross-linking towards flame retardance, first of all, cross-linking behaviors of P(ET-co-P)s were characterized using simultaneous Thermogravimetry – Differential Scanning Calorimetry (TG-DSC) in N<sub>2</sub> (Fig. 3). Detailed data are presented in Table 3. The behavior of PET was also measured for comparison. From the DSC thermogram for P(ET-co-P)<sub>20</sub>, the cross-linking reaction is apparent as a notable exothermic process starting at 340 °C, just between the melting (*c.a.* 220 °C) and the decomposition peak (*c.a.* 440 °C) [21–25]; while contrarily, neat PET directly decomposes after melting. It is clear that the cross-linking temperature is much higher than the melting point, which provides a broad temperature window for processing. For all the P(ET-co-P)s, these obvious cross-linking peaks could be observed and the size of the exothermic peaks increased gradually with the increase in the content of PEPE in the copolyester, indicating that the cross-linking effects were becoming more prominent. Also, as more PEPE was incorporated, the earlier cross-linking of copolyester occurred: the onset temperatures for the cross-linking exothermic peaks for P(ET-co-P)<sub>20</sub>, P(ET-co-P)<sub>40</sub> and P(ET-co-P)<sub>80</sub> were 340 °C, 314 °C and 300 °C, respectively. At the same time, the melting peak for P(ET-co-P)<sub>20</sub> shifted to the much lower temperature (the endothermic enthalpy attenuated as well); and the melting behavior could not be observed with a further increase in concentration of the functional monomer, reflecting the considerable diminishment of the crystalline phase of the copolyesters due to the bulky pendent phenylethynyl groups along the molecular chains [26,27]. Meanwhile, P(ET-co-P)<sub>40</sub> and P(ET-co-P)<sub>80</sub> both exhibited relatively low glass transition temperatures (T<sub>g</sub>), and their cross-linking temperatures were far above the processing temperature of a polyester. TGA curves showed the initial decomposition temperature (T<sub>5%</sub>, defined as the temperature of 5 wt% weight loss) of P(ET-co-P)s was always higher than the cross-

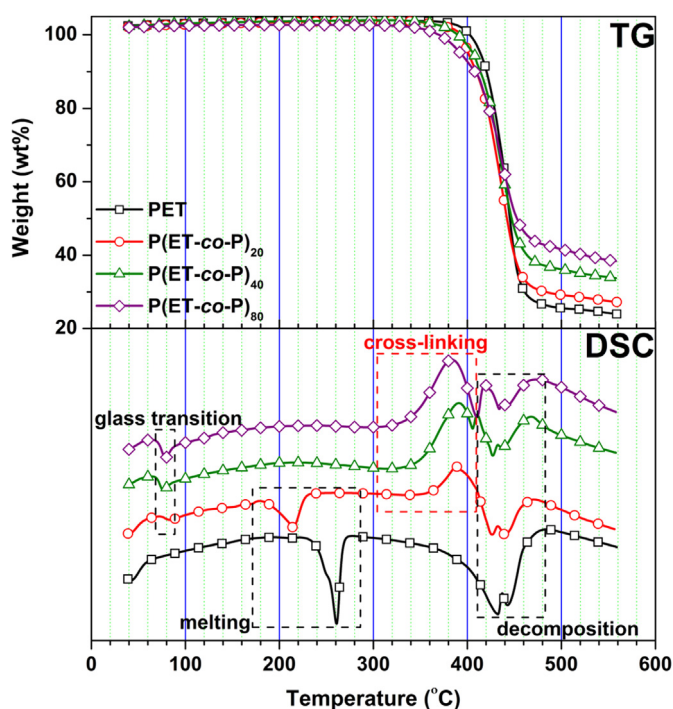


Fig. 3. TG-DSC thermograms for PET and P(ET-co-P) copolyesters at a heating rate of 10 °C min<sup>-1</sup> in N<sub>2</sub>.

Table 3  
TG-DSC data for PET and P(ET-co-P) copolyesters.

Samples	PET	P(ET-co-P) <sub>20</sub>	P(ET-co-P) <sub>40</sub>	P(ET-co-P) <sub>80</sub>
T <sub>g</sub> (°C)	76	76	80	82.1
T <sub>m</sub> (°C)	251	208	–	–
T <sub>c</sub> (°C) <sup>a</sup>	–	340	314	300
T <sub>5%</sub> (°C) <sup>b</sup>	417	407	406	393

<sup>a</sup> T<sub>c</sub> defined as the temperature at which the exothermic peak started.

<sup>b</sup> T<sub>5%</sub> defined as the temperature at which 5 wt% weight loss occurred.

linking temperature, indicating that the cross-linking reaction occurred prior to the decomposition. Taken together, this unique thermal property confirmed P(ET-co-P)s would conduct cross-linking reaction in the proper temperature range lower than the decomposition temperature but much above its processing temperature.

The cross-linking reaction of the phenylethynyl groups and the corresponding mode of action have been widely investigated. It is generally believed that the acromatization process occurs through a radical process. Reactions proposed include the formation of two phenylethynyl groups to one triphenyl naphthalene cross-links [28], which could play a positive effect on viscousing and further on anti-dripping.

It is easy to understand that the low melting viscosity is one of the direct causes of melt dripping: during combustion, a weak and thin melt couldn't support its own weight at the high temperature, thus melt dripping occurs. Moreover, a strong melt with large melting viscosity and strength could inhibit the proliferation of combustible gases, further to slow the combustion process [29–31]. As the most significant effect of such cross-linking, the increased complex viscosity ( $|\eta^*|$ ) of the copolyesters during the heating process was investigated by temperature-dependent dynamic oscillatory rheological measurements.

The temperature dependence on  $|\eta^*|$  for P(ET-co-P) copolyesters and neat PET is shown in Fig. 4. For neat PET,  $|\eta^*|$  singly showed a linear decrease during the heating process, which lead to serious melt dripping. However, the  $|\eta^*|$  of P(ET-co-P)s experienced a decrease firstly, then subsequently increased sharply from  $T_c$  (where  $|\eta^*|$  starts to increase, and the cross-linking reaction occurs [32,33]), and the 'U-shape' change could be clearly observed over the whole temperature range. This unusual rheological behavior could be explained as follows. Upon heating, the easier movement of polymer chains resulted in a decrease in  $|\eta^*|$  of the sample; however for P(ET-co-P)s, the abnormal increase of  $|\eta^*|$  was due to the occurrence of a cross-linking reaction or the reaction overwhelming the decomposition of the copolyester [34]. With the increase of PEPE content, the  $|\eta^*|$  of P(ET-co-P)s at 330 °C increased. According to the TG-DSC results, the content of PEPE directly determined the onset temperature ( $T_c$ ) and the degree of cross-linking reaction. However, different from the cross-linking reaction in nitrogen (TG-DSC), the initial cross-linking in air occurred earlier (still much higher than the processing temperature), which might be attributed to the participation of oxygen in cross-linking reaction. Consequently, the high  $|\eta^*|$  caused by cross-linking could effectively reduce the flammability of the copolyesters by suppressing the vigorous bubbling process in the course of

degradation during combustion, and simultaneously inhibit the melt dripping effectively as previously mentioned [29–31,34]. Thus, P(ET-co-P)s with higher content of PEPE exhibited a bigger  $|\eta^*|$ , leading to better flame-retardant and anti-dripping effects, which was in agreement with the result of the flammability tests.

The increasing rate of  $|\eta^*|$  ( $v_{\eta^*}$ ) at a constant temperature, as reflected to the cross-linking rate, was also investigated in detail, as summarized in Table 4. Fig. 4(b) contains  $|\eta^*|$  plots for PET and P(ET-co-P)s with different content of PEPE against time at 300 °C in an air atmosphere, and the effects of the content of PEPE on the cross-linking rate were studied. PET showed no increase in  $|\eta^*|$  over time; but all tested P(ET-co-P)s exhibited a good linear relationship between viscosity and time, and the rate of the complex viscosity increased with the increase of PEPE content. The different increasing rates of the complex viscosity reflecting to the rate of cross-linking should correlate with the relative concentrations of reactive phenylethynyl groups, and thus account for the different flame-retardant properties [25]. That is to say, time is a critical parameter for the increase of  $|\eta^*|$ , and P(ET-co-P)s with lower content of PEPE need longer time to reach the large melt viscosity. Consequently P(ET-co-P)s showed different flame-retardant effects using different burning tests, for each testing environment and combustion intensity were widely different. Therefore, P(ET-co-P)s even with very low content of PEPE exhibited a considerable flame retardance in cone calorimeter tests with the persistent external heat irradiation and attendant long heating duration, but showed poor effect in the UL-94 tests due to the short heating time.

A melt viscosity was the most important factor for facilitating anti-dripping, while it also played an important role in flame retardance of materials. But for extinguishment of materials, melt viscosity alone was not enough. The flame-retardant mode of action required further investigation.

### 3.3. Thermal stability and degradation

The thermal degradation behavior of the copolyesters was investigated in hope of finding the potential flame-retardant mode of action. Fig. 5 contains the thermogravimetric curves of PET and P(ET-co-P) copolyesters under nitrogen atmosphere before and after cross-linking. The  $T_{5\%}$ ,  $T_{max}$ , and residue for all samples after the tests are presented in Table 5. For PET and P(ET-co-P) copolyesters before cross-linking (Fig. 5a), all of the curves contain a similar major break. Incorporation of PEPE decreased the initial decomposition temperature:  $T_{5\%}$  of P(ET-co-P)s decreased from 372.5 °C to 369.2 °C (still much higher than the cross-linking temperature) with increase of PEPE content. More importantly,

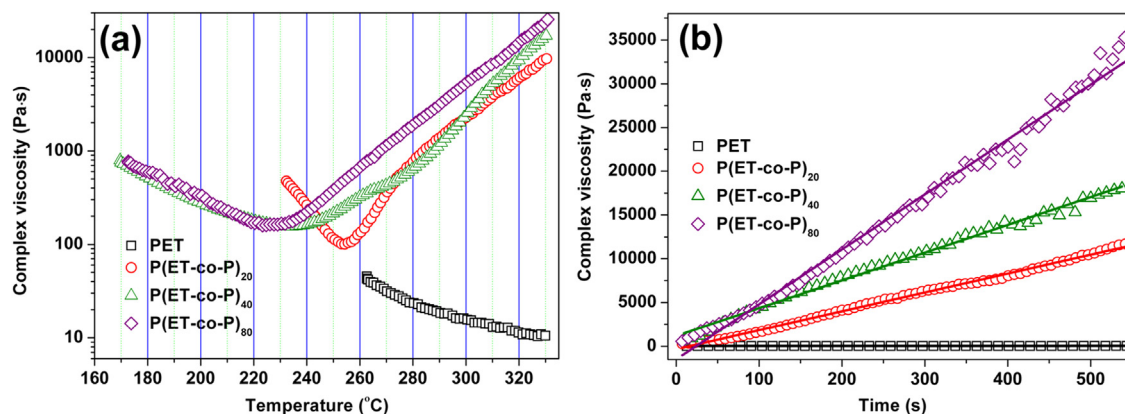


Fig. 4. Dynamic oscillatory rheological results for PET and P(ET-co-P) copolyesters in air atmosphere: (a) Complex melt viscosity plotted against temperature at a heating rate of 10 °C min<sup>-1</sup>; (b) Complex melt viscosity plotted against time at a fixed temperature of 300 °C.

**Table 4**  
Rheological data for PET and P(ET-co-P) copolyesters.

Samples	PET	P(ET-co-P) <sub>20</sub>	P(ET-co-P) <sub>40</sub>	P(ET-co-P) <sub>80</sub>
$r^2$	0.967	0.997	0.993	0.990
$v_{\eta}$ (Pa)	0.01	21.6	31.7	62.8

$r^2$  stands for the correlation coefficient of the linear relationship between complex melt viscosity and time.

$v_{\eta}$  stands for the increasing rate of  $|\eta^*|$  at 300 °C, as reflected to the cross-linking rate.

residual char from decomposition of P(ET-co-P)s increased considerably with an increase in PEPE content, which might be ascribed to an *in situ* cross-linking reaction (further aromatization to char formation) in competition with thermal degradation during the TGA testing process. Before massive thermal degradation, the cross-linking reaction of the copolyesters was dominant, and the cross-linked networks formed from this stage determine the final carbon residue (Fig. 6). P(ET-co-P)s with greater PEPE content had more efficacious cross-linking structures with faster cross-linking rates, consequently more residual char was obtained.

For better understanding, P(ET-co-P)s were first cross-linked at 320 °C for 60 min in air prior to the TGA tests, and the resulting thermograms are shown in Fig. 5(b). PET was also heat treated for comparison.

Compared with the decomposition of the original copolyesters,  $T_{5\%}$  for the cross-linked P(ET-co-P)s is significantly higher, suggesting the formation of the thermostable cross-linked structure which prevents early decomposition [35]. Furthermore, decomposition of the cross-linked P(ET-co-P)s produced much higher residual char than the original ones did, indicating that pre-formed cross-linked networks are thermally stable even at extremely high temperature, as previously reported [36,37]. These stable cross-linked networks might play a positive role in both flame retardance and anti-dripping of the copolyester. However, it's worthwhile to notice that, comparing the TGA thermograms for the copolyesters before and after pre-treated cross-linking, the *in situ* formed cross-linked structures exhibited limited efficiency on both thermal stability and flame retardance, due to the unsatisfied cross-linking rate, particularly for the copolyester with smaller amount of phenylethynyl group.

To further investigate the thermal degradation behavior of the resulting materials, TG-FTIR was used to study the gaseous products, which provided insight into the thermal degradation process. The gaseous products from the decomposition of PET and P(ET-co-P)<sub>40</sub> at different temperature are shown in Fig. 7. First of all, it is noteworthy that both FTIR spectra for volatile products up to 330 °C

**Table 5**  
TGA data for PET and P(ET-co-P) copolyesters before and after cross-linking.

Sample	Before cross-linking			After cross-linking		
	$T_{5\%}$ (°C) <sup>a</sup>	$T_{max}$ (°C) <sup>b</sup>	Residue at 700 °C (wt%)	$T_{5\%}$ (°C)	$T_{max}$ (°C)	Residue at 700 °C (wt%)
PET	396.7	432.5	11.5	387.5	435.0	8.9
P(ET-co-P) <sub>20</sub>	372.5	435.2	15.2	384.1	435.4	26.3
P(ET-co-P) <sub>40</sub>	364.7	436.2	19.6	391.0	436.6	30.6
P(ET-co-P) <sub>60</sub>	365.8	436.2	23.9	395.2	437.3	36.1
P(ET-co-P) <sub>80</sub>	369.2	436.2	28.5	390.0	434.9	38.0

<sup>a</sup>  $T_{5\%}$  defined as the temperature at which 5 wt% weight loss occurred.

<sup>b</sup>  $T_{max}$  defined as the temperature at maximum weight loss rate.

contain no absorption other than those traces of H<sub>2</sub>O and CO<sub>2</sub>. This suggests that decomposition did not occur and the cross-linking of the copolyester was the major reaction to this point. For further degradation at higher temperature, there was no significant difference in products formed between P(ET-co-P)<sub>40</sub> and PET. The spectra for the evolved gaseous products, in both cases, exhibited characteristic bands for aliphatic ethers (1100–1250 cm<sup>-1</sup>), benzoic acid and RCHO (1760 and 2734 cm<sup>-1</sup>), CO (2108 cm<sup>-1</sup>), CO<sub>2</sub> (2357 and 668 cm<sup>-1</sup>), hydrocarbons (2820–2980 cm<sup>-1</sup> and 1300–1450 cm<sup>-1</sup>) and H<sub>2</sub>O. The decomposition products were in accordance with those observed previously for the decomposition of PET [38,39]. Consequently, the cross-linked structure and pre-formed cross-linked networks did not fundamentally change the composition of evolved products in the gaseous phase, P(ET-co-P)s exhibited similar chain scission and decomposition process as did PET after cross-linking, and the flame-retardant action of copolyesters was mostly a condensed phase phenomenon.

Even if the composition of gaseous products from the decomposition of P(ET-co-P)s was almost the same as that from PET, the carbonization process of the copolyester was rather complicated and was tracked by XPS in this paper. The C<sub>1s</sub> XPS results for the heat treated P(ET-co-P)<sub>40</sub> were presented in Table 6. With the increase of temperature, the C/O ratios for P(ET-co-P)<sub>40</sub> gradually increased, suggesting that the carbonization process was decarboxylation process or aromatization process. The extent of aromatization was different at different temperature. C<sub>ox</sub> stands for the oxidized carbons, while C<sub>a</sub> denotes the aliphatic and aromatic carbons, which represents more contacts between carbon atoms. The smaller C<sub>ox</sub>/C<sub>a</sub> means the bigger condensation degree of the aromatic species [40]. From Table 6, C<sub>ox</sub>/C<sub>a</sub> decreased with the increase of temperature during the degradation process, which further indicated that the carbonization process was the

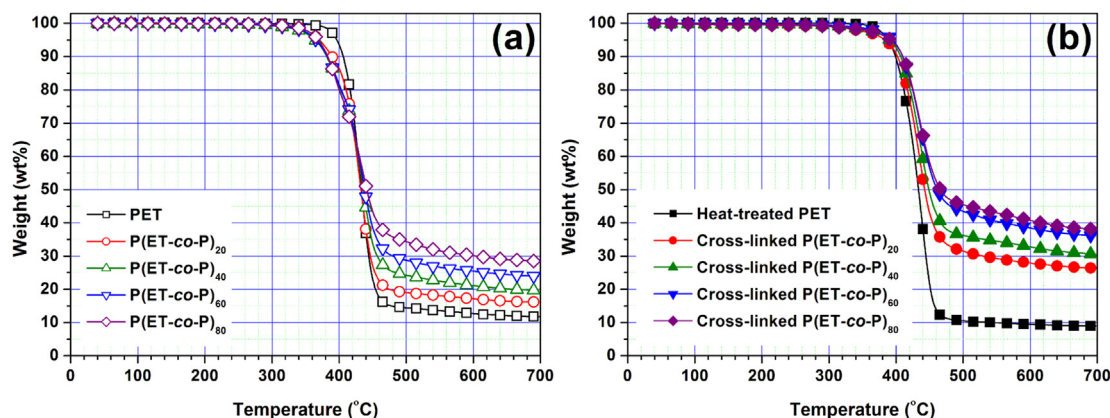


**Fig. 5.** TGA thermograms for PET and P(ET-co-P) copolyesters before (a) and after cross-linking (b) (cross-linked at 320 °C for 60 min for P(ET-co-P) copolyesters, for comparison, PET was thermally treated in the same way) in nitrogen atmosphere at heating rate of 10 °C min<sup>-1</sup>.

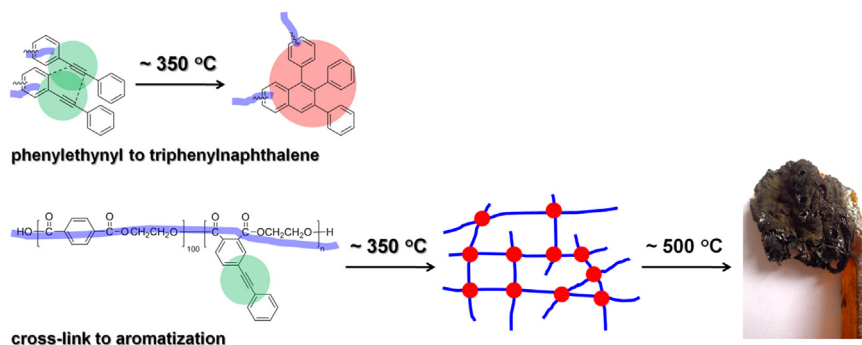


Fig. 6. Thermal degradation and carbonization process for P(ET-co-P) copolyesters.

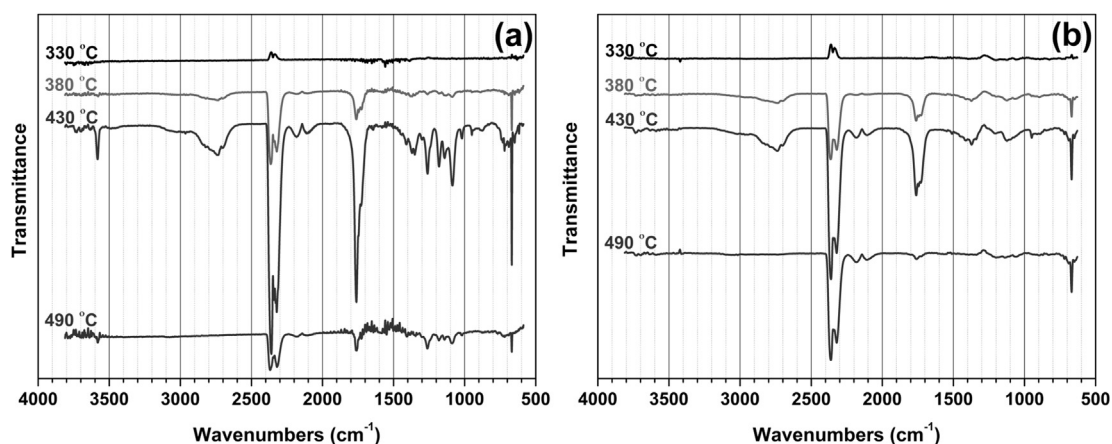


Fig. 7. FTIR spectra for pyrolysis products from the decomposition of neat PET (a) and P(ET-co-P)<sub>40</sub> (b) at different temperatures.

aromatization-dominant process. Thus, carbonaceous materials of the copolyester are composed mainly of polyaromatic species formed during the thermal degradation process, which would play an important role in self extinguishment and flame inhibition during combustion.

### 3.4. Char formation

As for the typical action of the charring flame retardant, the compact char layer formed during burning is very important for material self-extinguishing. This critical layer prohibits the combustible volatiles generated from decomposition of polymers entering the flame zone, and also prevents the transfer of heat and oxygen [41]. Therefore, in order to investigate the relationships between the cross-linked structure and char formation, as well as the flame-retardant mode of action, the structures and morphologies for the residue char from composites after cone calorimeter tests were studied in detail [42,43].

**Table 6**  
Results of C1s XPS for the heat treated P(ET-co-P)<sub>40</sub> at different temperatures.

Temperature (°C)	C–C area (%)	C–O area (%)	C=O area (%)	C(O)O area (%)	C/O	C <sub>ox</sub> /C <sub>a</sub> <sup>a</sup>
330	64.5	24.8	0	10.7	3.8	0.55
380	66.1	19.9	5.5	8.5	5.5	0.51
430	67.0	19.9	5.5	7.5	10.0	0.49
550	67.7	20.9	6.2	5.2	10.9	0.47

<sup>a</sup> C<sub>ox</sub> stands for the oxidized carbons; C<sub>a</sub> denotes the aliphatic and aromatic carbons.

The chemical constitution of the charring residue after cone calorimetric tests for PET, P(ET-co-P)<sub>40</sub> and P(ET-co-P)<sub>80</sub> were investigated by XPS. The detailed data are presented in Table 7. Compared with neat PET, P(ET-co-P)s have lower C/O ratios, which may be caused by that oxygen participated in the cross-linking of the phenylethynyl at early stage of combustion; but the specific reason is not fully understood. However, it is interesting that C<sub>ox</sub>/C<sub>a</sub> ratios for P(ET-co-P)s are also lower than that of neat PET, which indicates that P(ET-co-P)s had more polyaromatic species from their cross-linked structures. More polyaromatic species mean denser morphology, better barrier effect and flame retardance. The polyaromatic cross-linked networks are the foundations that make materials extinguish in the fire.

The surface morphology, as an important criterion to define the efficacy of a flame retardant to the char formation, was investigated by SEM. The detailed images are shown in Fig. 8. For neat PET, it could be seen that the residue was a fractured char with lots of flaws and pores on its surface, and was susceptible to cracking in burning. But for P(ET-co-P)s, the SEM images (Fig. 8b–d) showed that very compact char residue was formed just like rough

**Table 7**  
Results of C1s XPS for residual char after cone for neat PET and P(ET-co-P) copolyesters.

Temperature (°C)	C–C area (%)	C–O area (%)	C=O area (%)	C(O)O area (%)	C/O	C <sub>ox</sub> /C <sub>a</sub>
PET	63.5	21.9	8.2	6.5	7.6	0.58
P(ET-co-P) <sub>40</sub>	65.6	23.9	5.7	4.8	5.8	0.52
P(ET-co-P) <sub>80</sub>	65.6	21.8	7.6	5.0	6.7	0.52

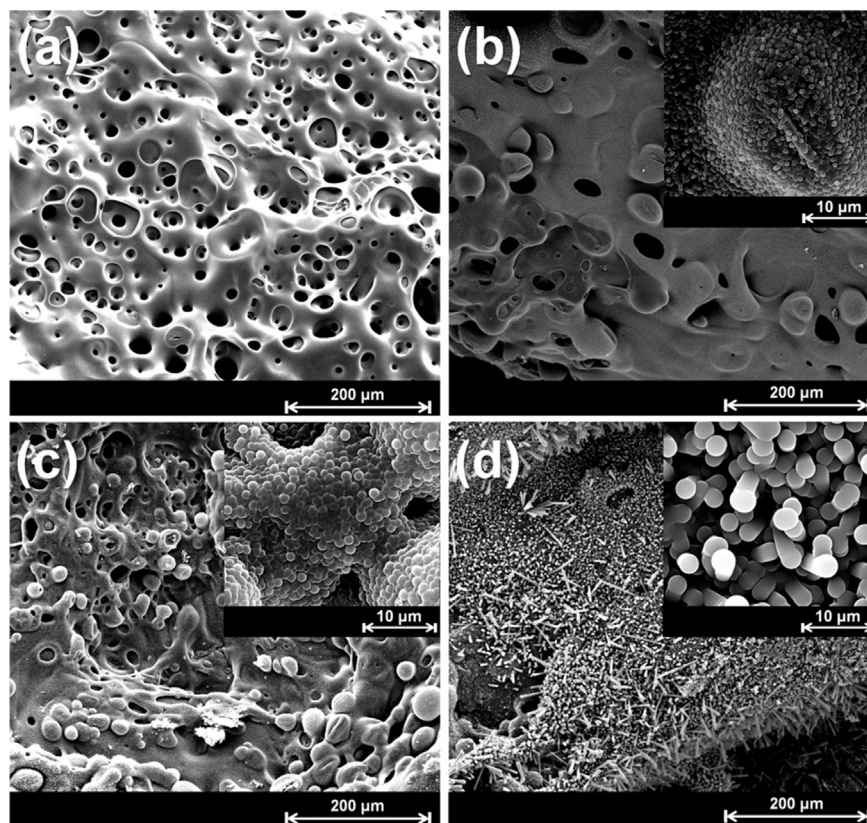


Fig. 8. SEM images for the char residue after cone calorimeter tests for PET and P(ET-co-P) copolyesters: (a) neat PET, (b) P(ET-co-P)<sub>20</sub>, (c) P(ET-co-P)<sub>40</sub>, (d) P(ET-co-P)<sub>80</sub>.

“carbonaceous clothes” coated at the surface; and these char became more compact with an increase in PEPE content, corresponding to better flame retardance and self extinguishing behavior. Especially for P(ET-co-P)<sub>80</sub> from Fig. 8d, an acicular “carbonaceous cloth” with few pores was found, which could provide a best barrier to avoid the transfer of heat and combustible gases. Interestingly, these closely packed acicular chars had regular cylindrical shape with very uniform sizes about 2 μm (Fig. 8d). Other P(ET-co-P)s also possessed special and fine surface morphologies for residue char, while these morphologies were very different depending on the PEPE content. Compared with the regular cylinder for P(ET-co-P)<sub>80</sub>, a spherical cell structure with uniform sizes was observed for P(ET-co-P)<sub>20</sub> and P(ET-co-P)<sub>40</sub>, and their sizes were 500 nm and 1 μm respectively. The granular surface of the residual char for P(ET-co-P)s exhibited more independent arrangement with an increase in PEPE content, and each independent granule got much bigger. But overall, the number of cavities and pores on the charring surface decreased with an increase in PEPE content. Thus, the copolyester with higher content of the cross-linkable monomer exhibits better flame-retardant and self-extinguishing effect, as well as anti-dripping performance.

Raman spectroscopy provides a suitable method to characterize the different types of carbonaceous materials, particularly for the carbonaceous materials formed during combustion [44,45]. In this manuscript, the residual chars for neat PET, P(ET-co-P)<sub>40</sub>, and P(ET-co-P)<sub>80</sub> after cone calorimetric analysis were inspected. As shown in Fig. 9, the spectra for all testing samples exhibited overlapping peaks with intensity maxima at about 1580 cm<sup>-1</sup> and 1360 cm<sup>-1</sup>, which were the typical polyaromatic species or so-called graphitic structures. The first band (called the G band) corresponds to the stretching vibration mode with E<sub>2g</sub> symmetry in the sp<sup>2</sup> hybridized carbon atoms in a graphite layer, whereas the latter one (called the

D band) represents disordered graphite or glassy carbons [46]. More importantly, according to the statement of Tuinstra and Koenig, the relative ratio of the integrated intensities of D and G bands ( $I_D/I_G$ ) was inversely proportional to an in-plane microcrystalline size, where  $I_D$  and  $I_G$  were the integrated intensities of D and G bands, respectively [47,48]. As shown in Fig. 9, each spectrum was subjected to peak fitting using the curve fitting software Origin 8.0/ Peak Fitting Module to resolve the curve into 2 Gaussian bands. Basically, the bigger the ratio of  $I_D/I_G$  is, the smaller size of carbonaceous microstructures is, which means better flame retardance, as the report elsewhere [49]. From Fig. 9, the  $I_D/I_G$  ratio followed the sequence of PET (1.26) < P(ET-co-P)<sub>40</sub> (1.88) < P(ET-co-P)<sub>80</sub> (2.50), indicating the copolyester with the highest cross-linked density possessed the smallest carbonaceous microstructure, the best flame retardance and anti-dripping performance. The results of Raman, XPS, and SEM are further in agreement with the fire test results.

### 3.5. Description of the flame-retardant process

Overall, the flame-retardant processes for P(ET-co-P)s could be speculated as follows (Fig. 6): firstly, P(ET-co-P)s underwent quick cross-linking process when the materials were ignited; then, the formed stable cross-linked networks resulted in the increase of melt viscosity. On the one hand, the huge melt viscosity prevented the melt-dripping to occur, meanwhile the proliferation of combustible gases were also inhibited by the large melt viscosity, further to slow the combustion process. On the other hand, the cross-linked networks would not change the evolved products in the gaseous phase but make a great contribution to the residual char of which the content, chemical composition and the surface morphology were all affected. At last, the residual char constituted

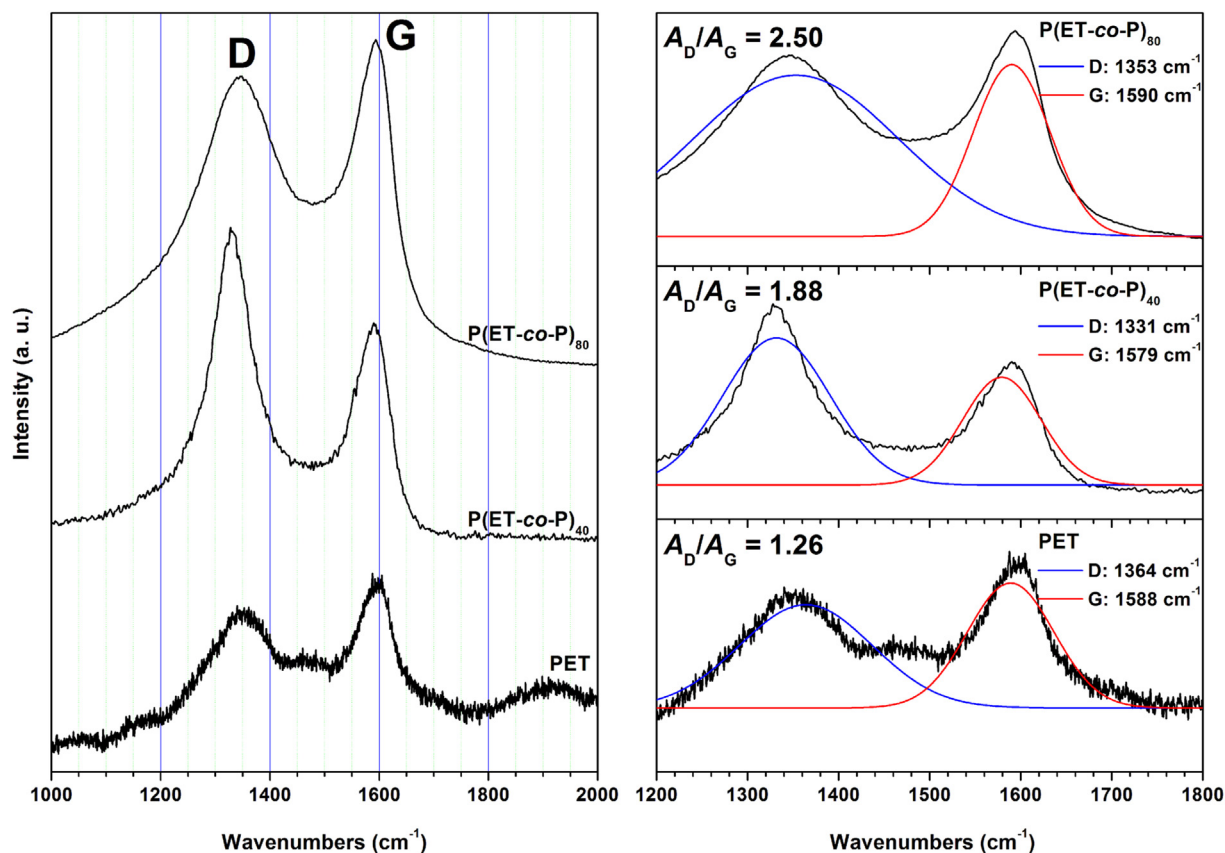


Fig. 9. Raman spectra for the char residue after cone calorimeter tests analyses for PET and P(ET-co-P) copolyesters.

mainly of polyaromatic species was formed, and its microstructural size was extremely small, which made the char very dense and compact. The char layer prevented the transfer of heat, oxygen and combustible volatiles, and finally made fire go out.

#### 4. Conclusion

The novel high-temperature crosslinkable copolyesters with high content of cross-linking monomers have been synthesized, and their flammability, anti-dripping performances, especially the corresponding mode of action was investigated in detail. The flammability results suggested P(ET-co-P) copolyesters with high content of PEPE not only had good performance in the cone, but also passed the traditional flame retardance tests such as UL 94 (V-0) and LOI tests, while the melt-dripping was totally inhibited. TG-DSC, TGA and rheological analysis were used to investigate the thermal cross-linking behavior of copolyester, and proved that the degree and rate of cross-linking reaction were determined by the content of functional monomer PEPE. The rheological analysis showed that the melt viscosity of P(ET-co-P)s increased sharply during the heat process, and the huge melt viscosity played an important role in inhibiting the combustion and avoiding the melt-dripping. Consequently, cross-linking rate of copolymer and the extent of cross-linking reaction together determined the flame-retardant effect of copolyesters during burning.

The results of the thermal degradation analysis indicated that the formed cross-linked networks did not change the composition of evolved products in the gaseous phase but promoted the further formation of residual char, indicating the flame-retardant action of copolyesters was condensed phase-dominant. XPS, SEM and Raman analysis suggested that the char layers were constituted

mainly of polyaromatic species with small and uniform microstructures at the surface. Both the large melt viscosity and the formation of an especially compact char with fine microstructure resulting from cross-linking were considered as the key points to the flame retardance and anti-dripping performance of the polymer when subjected to the flame.

#### Acknowledgments

Financial supports by the National Natural Science Foundation of China (Grant Nos. 50933005, 51121001), Program for Changjiang Scholars and Innovative Research Team in University (IRT. 1026) would be sincerely acknowledged. The authors would also like to thank the Analysis and Testing Center of Sichuan University for the NMR and Raman measurements.

#### References

- [1] Li YC, Mannen S, Morgan AB, Chang SC, Yang YH, Condon B, et al. *Adv Mater* 2011;23(34):3926–31.
- [2] Yang R, Chen L, Zhang WQ, Chen HB, Wang YZ. *Polymer* 2011;52(18):4150–7.
- [3] Blum A, Ames BN. *Science* 1977;195(4273):17–23.
- [4] Chen L, Huang HZ, Wang YZ, Jow J, Su K. *Polymer* 2009;50(13):3037–46.
- [5] Chen L, Wang YZ. *Polym Adv Technol* 2010;21(1):1–26.
- [6] Wu CS, Liu YL, Chiu YS. *Polymer* 2002;43(15):4277–84.
- [7] Hayashida K, Tsuge S, Ohtani H. *Polymer* 2003;44(19):5611–6.
- [8] Hsieh CY, Su WC, Wu CS, Lin LK, Hsu KY, Liu YL. *Polymer* 2013;54(12):2945–51.
- [9] Lin CH, Chen CJ, Huang CM, Jehng JM, Chang HC, Juang TY, et al. *Polymer* 2013;54(26):6936–41.
- [10] Ellzey KA, Ranganathan T, Zilberman J, Coughlin EB, Farris RJ, Emrick T. *Macromolecules* 2006;39(10):3553–8.
- [11] Ryu BY, Moon S, Kosif I, Ranganathan T, Farris RJ, Emrick T. *Polymer* 2009;50(3):767–74.

- [12] Zhao HB, Chen L, Yang JC, Ge XG, Wang YZ. *J Mater Chem* 2012;22(37):19839–57.
- [13] Chen HB, Hollinger E, Wang YZ, Schiraldi DA. *Polymer* 2014;55(1):380–4.
- [14] Weil ED, Hirschler MH, Patel NG, Said MM, Shakir S. *Fire Mater* 1992;16(4):159–67.
- [15] Wilkie CA, Chigwada G, Gilman JW, Lyon RE. *J Mater Chem* 2006;16(21):2023–30.
- [16] Bourbigot S, Flambard X. *Fire Mater* 2002;26(6):155–68.
- [17] Northolt MG, Sikkema DJ, Zegers HC, Klop EA. *Fire Mater* 2002;26(6):169–72.
- [18] Wang JS, Zhao HB, Ge XG, Liu Y, Chen L, Wang DY, et al. *Ind Eng Chem Res* 2010;49(9):4190–6.
- [19] Ge XG, Wang C, Hu Z, Xiang X, Wang JS, Wang DY, et al. *J Polym Sci Part A Polym Chem* 2008;46(9):2994–3006.
- [20] Wang YZ. *Flame-retardation design of PET fibres*. Chengdu: Sichuan Science and Technology Press; 1994.
- [21] Johnston JA, Li FM, Harris FW, Takekoshi T. *Polymer* 1994;35(22):4865–73.
- [22] Meyer GW, Glass TE, Grubbs HJ, McGrath JE. *J Polym Sci Polym Chem* 1995;33(13):2141–9.
- [23] Li WW, Tang HY, Chen XF, Fan XH, Shen ZH, Zhou QF. *Polymer* 2008;49(19):4080–6.
- [24] Gong C, Luo Q, Li Y, Giotto M, Cilpllini NE, Yang Z, et al. *J Polym Sci Polym Chem* 2010;48(18):3950–63.
- [25] Drake K, Mukherjee I, Mirza K, Ji HF, Wei Y. *Macromolecules* 2011;44(11):4107–15.
- [26] Chen HB, Chen L, Zhang Y, Zhang JJ, Wang YZ. *Phys Chem Chem Phys* 2011;13(23):11067–75.
- [27] Chen HB, Zeng JB, Dong X, Chen L, Wang YZ. *CrystEngComm* 2013;15(14):2688–98.
- [28] Fang XM, Xie XQ, Simone CD, Stevens MP, Scola DA. *Macromolecules* 2000;33(5):1671–81.
- [29] Kashiwagi T, Du FM, Douglas JF, Winey KI, Harris RH, Shield JR. *Nat Mater* 2005;4(12):928–33.
- [30] Kashiwagi T, Grulke E, Hilding J, Groth KM, Harris RH, Butler K, et al. *Polymer* 2004;45(12):4227–39.
- [31] Kashiwagi T, Du FM, Winey KI, Groth KM, Shields JR, Bellayer SP, et al. *Polymer* 2005;46(2):471–81.
- [32] Song PA, Liu H, Shen Y, Du B, Fang ZP, Wu Y. *J Mater Chem* 2009;19(9):1305–13.
- [33] Song PA, Zhao L, Cao Z, Fang ZP. *J Mater Chem* 2011;21(21):7782–8.
- [34] Song PA, Zhu Y, Tong LF, Fang ZP. *Nanotechnology* 2008;19(22):225707–16.
- [35] Yang LQ, He B, Meng S, Zhang ZJ, Li M, Guo J, et al. *Polymer* 2013;54(11):2668–75.
- [36] Meador MA. *Ann Rev Mater Sci* 1998;28(1):599–630.
- [37] Holland TV, Glass TE. *Polymer* 2000;41(13):4965–90.
- [38] Deng Y, Zhao CS, Wang YZ. *Polym Degrad Stab* 2008;93(11):2066–70.
- [39] Yang W, Song L, Hu Y, Lu HD, Yuen RKK. *Compos Part B* 2011;42(5):1057–65.
- [40] Bourbigot S, Bras ML, Delobel R, Gengembre L. *Appl Surf Sci* 1997;120(1):15–29.
- [41] Song PA, Xu LH, Guo ZG, Zhang Y, Fang ZP. *J Mater Chem* 2008;18(42):5083–91.
- [42] Pack SC, Bobo E, Muir N, Yang K, Swaraj S, Ade H, et al. *Polymer* 2012;53(21):4787–99.
- [43] Qian LJ, Feng FF, Tang S. *Polymer* 2014;55(1):95–101.
- [44] Sadezky A, Muckenhuber H, Grothe H, Niessner R, Pöschl U. *Carbon* 2005;43(8):1731–42.
- [45] Li L, Wei P, Li J. *J Fire Sci* 2010;28(6):523–38.
- [46] Tai Q, Hu Y, Yuen RKK, Song L, Lu HD. *J Mater Chem* 2011;21(18):6621–7.
- [47] Tuinstra F, Koenig JL. *J Chem Phys* 1970;53(3):1126–30.
- [48] Ferrari AC, Robertson J. *Phys Rev B* 2000;61(20):14095–107.
- [49] Bourbigot S, Bras ML, Delobel R, Decressain R, Amoureux JP. *J Chem Soc Faraday Trans* 1996;92(1):149–58.